Physical properties, spectral reflectance and thickness development of first year fast ice in Kongsfjorden, Svalbard

Sebastian Gerland, Jan-Gunnar Winther, Jon Børre Ørbæk & Boris V. Ivanov

A ground truth study was performed on first year fast ice in Kongsfjorden, Svalbard, during spring 1997 and 1998. The survey included sea ice thickness monitoring as well as observation of surface albedo, attenuation of optical radiation in the ice, physical properties and texture of snow and sea ice. The average total sea ice thickness in May was about 0.9 m, including a 0.2 m thick snow layer on top. Within a few weeks in both years, the snow melted almost completely, whereas the ice thickness decreased by not more than 0.05 m. During spring, the lower part of the snow refroze into a solid layer. The sea ice became more porous. Temperatures in the sea ice increased and the measurable salinity of the sea ice decreased with time. Due to snow cover thinning and snow grain growth, maximum surface albedo decreased from 0.96 to 0.74. Texture analysis on cores showed columnar ice with large crystals (max. crystal length >0.1 m) below a 0.11 m thick mixed surface layer of granular ice with smaller crystals. In both years, we observed sea ice algae at the bottom part of the ice. This layer has a significant effect on the radiation transmissivity.

S. Gerland, J.-G. Winther & J. B. Ørbæk, Norwegian Polar Institute, Polar Environmental Centre, N-9296 Tromsø, Norway; B. V. Ivanov, Arctic and Antarctic Research Institute, Bering 38, 199397 St. Petersburg, Russia.

Introduction

Many publications (e.g. Wadhams 1994) underline the importance of sea ice for climate-related research. Climate modelling and remote sensing studies of sea ice rely heavily on ground truth data from field measurements. Knowledge of the physical properties and thickness of sea ice and its snow cover are crucial for understanding reflectance characteristics, energy balance, and marine biological productivity.

Ice thickness measurements from surface, ships or air (e.g. Kovacs & Morey 1991; Wadhams 1994, Haas et al. 1997; Haas 1998; Vinje et al. 1998) usually give snapshot-like information on ice thickness. Due to limited accessibility and ice dynamics, it is difficult to obtain time series of ground truth data, including ice thickness and physical properties measured from the surface, especially during melting.

Optical properties of sea ice have interested researchers for several decades (e.g. Langleben 1968; Perovich 1994; Perovich, Roesler et al. 1998). The basic theory and physical principles of radiation measurements over snow-covered ground have been delineated (e.g. Wiscombe & Warren 1980; Warren 1982). Spectral characteristics of tundra snow before and after the onset of melt in spring in the Kongsfjorden area have been published (Gerland et al. 1999; Winther et al. 1999). The crucial role that Svalbard's seasonally ice-covered fiords play in the biological productivity dynamics has also been discussed (e.g. Mehlum 1991). For example, sea ice algae survival depends on radiation penetrating the sea ice and the physical and chemical properties of the water below the sea ice and within brine drainage channels (e.g. Ackley et al. 1979; Horner 1985).

This paper describes the changes of fast ice at Dyrevika in inner Kongsfjorden on the western coast of Svalbard at 79°N during the spring melts in 1997 and 1998 (Fig. 1). The survey included sea ice thickness monitoring, surface albedo and transmissivity measurements, logging of physical properties of snow and sea ice, as well as texture analysis of sea ice cores from thick and thin

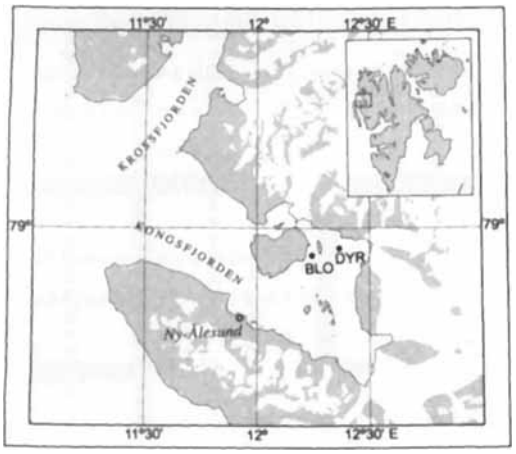

Fig. 1. Map of Kongsfjorden showing the research sites DYR and BLO. The Svalbard archipelago is shown in the inset. The settlement Ny-Ålesund is located at the southern coast of Kongsfjorden. Most of the studies presented here were performed at site DYR.

sections. Some work on sea ice in Kongsfjorden has been published. Carrying out biological studies in Kongsfjorden, Smith & Lydersen (1991) measured snow thickness on the sea ice. There are also published data on the extent of sea ice (spring seasons 1981–83, 1985–86, Mehlum 1991; spring 1984; Smith & Lydersen 1991), showing that the break up of the sea ice cover in Kongsfjorden varies between April and July. Even as late as in July, these records show Dyrevika to be ice-covered, as this place is fairly well-protected by the surrounding coast (Fig. 1).

Methods and instrumentation

Most results presented here originate from measurements and sampling at site DYR (Dyrevika; Fig. 1). Samples were also taken once in 1997 from the fast ice edge off Blomstrandhalvøya (site BLO), about 2.5 km west of DYR. Long-term meteorological records from Ny-Ålesund, some 12 km south-west of Dyrevika, show a mean annual precipitation of 402.9 mm water equivalent (period 1975–1996), and mean annual temperature of −5.8°C (1935–1996, Førland et al. 1997).

Field work was performed from early May to mid-June. Continuous temperature and global radiation data were acquired at DYR with an automatic logging station, using standard thermometers and pyranometers. DYR was visited about three times a week. We monitored the thickness of snow and sea ice using drilling and snow stakes as well as a portable electromagnetic device (EM31, Geonics, Mississauga, Canada). This inductive method enables indirect, fast and non-destructive ice thickness determination (Kovacs & Morey 1991; Haas et al. 1997). Snow and sea ice temperature was measured with an electronic Pt100 thermometer. Snow density was recorded volumetrically using a half-litre tube and a spring balance. We made stratigraphic descriptions of the surface snow layer, including grain size determination, using a magnifying glass and a mm-scale pad. Sea ice cores were obtained with a drill that produces cores of about 0.1 m diameter. Ice core temperature was measured in holes drilled from the side into the core. Core pieces were melted for salinity determination with a standard conductivity meter. From two ice cores we prepared thick and thin sections in the cold laboratory at the Alfred Wegener Institute for Polar and Marine Research.

For spectral surface albedo determination we used a portable Fieldspec FR spectroradiometer (ASD, Boulder, USA). It measures over a wavelength range from 350 to 2500 nm. The field of view for the albedo measurements was 18°. The albedo set-up and instrumentation is described in Gerland et al. (1999). For the underwater measurements, a waterproof extension fibre was connected to a cosine receptor, mounted on swing arm, which could be operated through drill holes (construction like in Mobley et al. 1998). After lowering the sensor in a drill hole, the arm was swung up 90° such that the sensor was positioned a few centimetres below the sea ice and about one metre horizontally away from the drill hole.

Results

Meteorology: Results from the logging station set-up at DYR showed that the maximum short-wave global radiation typically varied from 300 Wm^{-2} (noon) for overcast conditions, which were more common, to 600 Wm^{-2} for clear skies. The average air temperature at DYR remained below 0°C in May, except for short warm periods during the first half of the month each year. The air temperature varied on average between −6 and +1°C, approaching 0°C at the end of May. In both

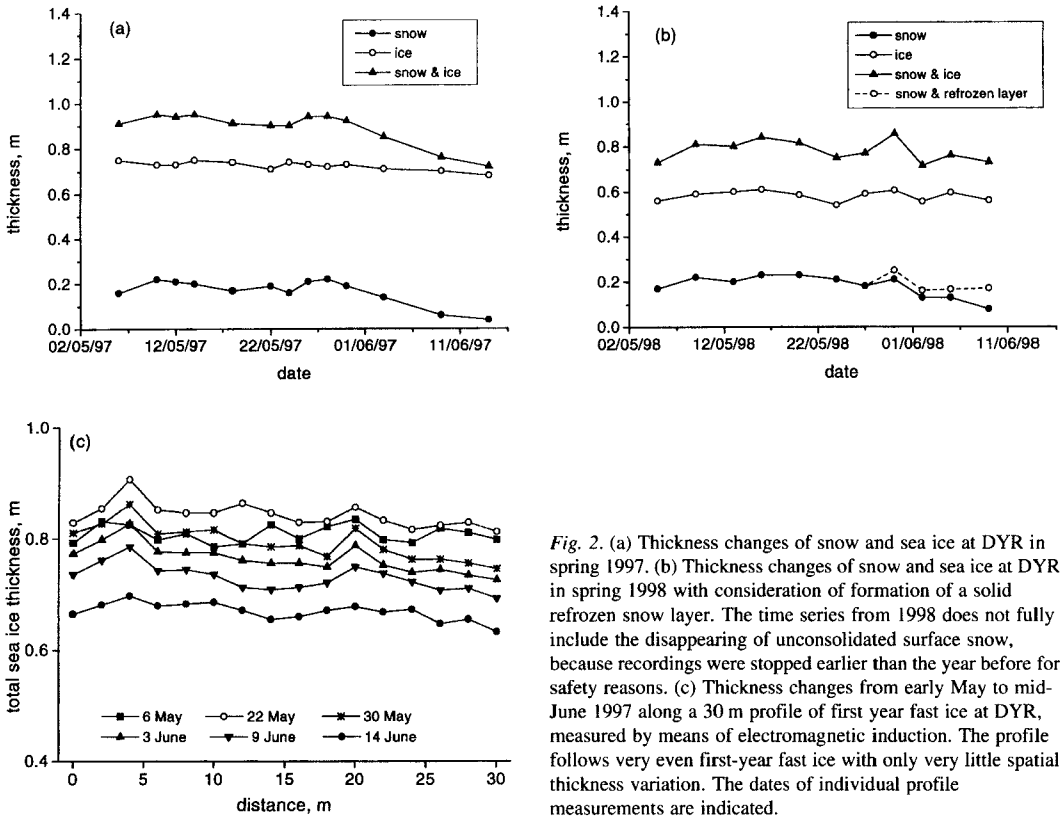

Fig. 2. (a) Thickness changes of snow and sea ice at DYR in spring 1997. (b) Thickness changes of snow and sea ice at DYR in spring 1998 with consideration of formation of a solid refrozen snow layer. The time series from 1998 does not fully include the disappearing of unconsolidated surface snow, because recordings were stopped earlier than the year before for safety reasons. (c) Thickness changes from early May to mid-June 1997 along a 30 m profile of first year fast ice at DYR, measured by means of electromagnetic induction. The profile follows very even first-year fast ice with only very little spatial thickness variation. The dates of individual profile measurements are indicated.

years, warm days with average air temperatures up to +2°C and intensive surface melting occurred during the last days of the measurements in early June. Integrated short-wave albedo at DYR decreased from around 0.8 in the beginning of May to 0.7 and below at the end of May and beginning of June. Similar values were measured in Ny-Ålesund, but there the albedo started to decrease later than on the fast ice, probably due to about twice the snow thickness (Gerland et al. 1999), and different snow temperatures and metamorphism compared with the sea ice.

Thickness monitoring: Most of the sea ice cover was very even and regular, apart from some encapsulated ice blocks originating from calving events from surrounding glaciers. The average total sea ice thickness in May 1997 was about 0.9 m, of which the top 0.2 m was snow. At the end of May and the beginning of June, the snow layer on top of the ice melted rapidly and almost completely, whereas the ice underneath decreased by only about 0.05 m (Fig. 2a). However, samples from drilling showed that, at the same time, the ice became very porous and thus lost strength (see texture analysis below).

The development of a solid layer of refrozen snow (see below) at the snow–sea ice interface made it difficult to define exactly the bottom of the snow layer. In 1998, we investigated this more closely and made distinctions between measurements which both included and excluded the refrozen snow layer (Fig. 2b). The initial total sea ice thickness in May 1998 was about 0.1 m less than the year before. This might be connected with the timing variability of onset of sea ice formation in winter.

Electromagnetic measurements, giving information on spatial variability and changes of total sea ice thickness with time, were taken along a 30 m long profile in 1997 (Fig. 2c). Using a conversion algorithm (Haas et al. 1997), total ice thickness was calculated from measured apparent electrical conductivity. The selected profiles show that the first significant thickness changes could be observed on 30 May 1997. The major thickness change is connected to snow thickness reduction, which was also observed by punctual

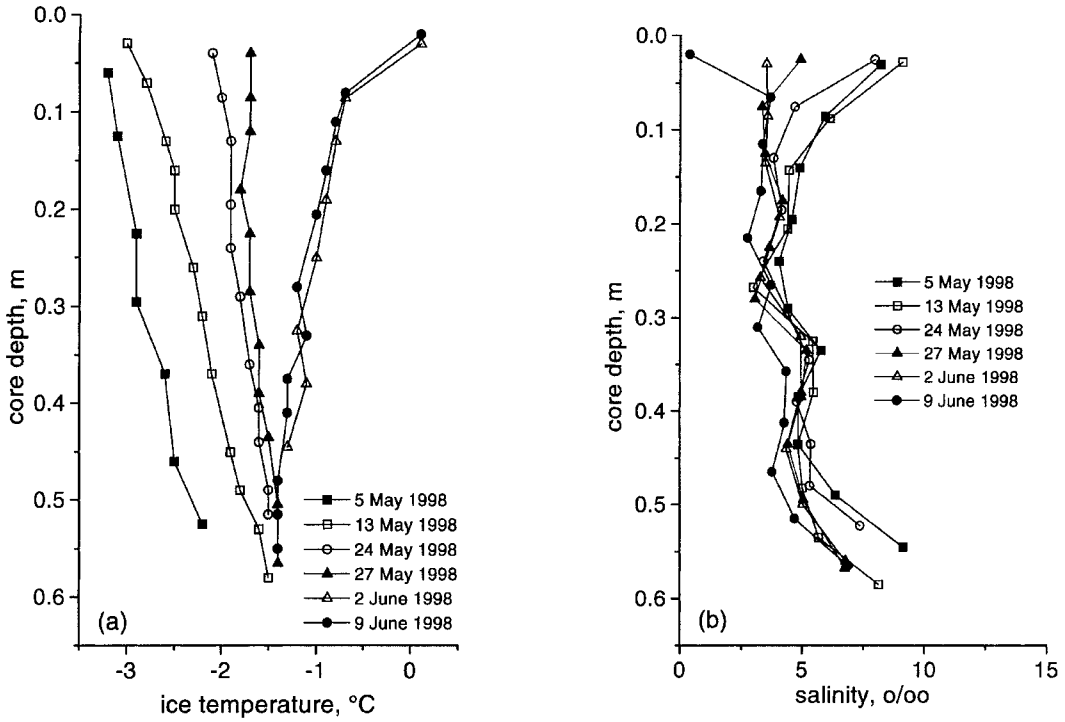

Fig. 3. Logs from ice cores obtained at DYR in spring 1998 (the dates of individual logs are indicated): (a) temperature, measured in small drill holes in the core, directly after obtaining the core; (b) salinity, measured from melted core sections.

direct surface measurements (Fig. 2a). A total thickness change (ice and snow) of about 0.2 m, derived from electromagnetics, accords with the direct measurements on snow and in boreholes (Fig. 2a).

Temperature and salinity: Snow and sea ice temperatures rose significantly through springtime. Figure 3a shows six selected temperature profiles from ice core measurements from spring 1998. While the logs from May show continuous warming with time, in June the temperature remained rather constant after reaching a certain level.

Before the onset of melting, salinity measurements on melted core samples show a typical C-shape (Fig. 3b), as it is known from other studies on first year sea ice (e.g. Clarke & Ackley 1984; Eicken, Lange & Dieckmann 1991; Perovich, Roesler et al. 1998). With warming, the salinity decreased in the upper part of the sea ice, probably due to wicking at the snow–ice interface (see refrozen snow, below) and loss of brine due to enlarged brine channels.

Snow: As a rule, snow grain sizes increase due to constructive and firnification metamorphosis, whereas precipitation events and destructive metamorphism produce finer grained snow (LaChapelle 1992). Average grain diameters of the surface snow at DYR increased from between 0.2 and 0.5 mm in early May to between 0.75 and 1 mm, occasionally up to 1.5 mm or more. In June, grain sizes in snow below the surface were even bigger, reaching 5 mm and more. In general, grain size increase reduces surface albedo (e.g. Wiscombe & Warren 1980). The freeboard (elevation of upper ice edge relative to water level) in early May was between +10 and −20 mm; later, after the onset of melt, it decreased to −40 mm. Reasons for this change were possibly density increase of surface snow and reduction of absolute ice volume due to melting and increased ice porosity.

Refrozen snow: From end of May onwards, we observed a slushy layer at the snow–sea ice interface and also a refrozen, 40 mm thick solid "snow" layer, here referred to as "refrozen

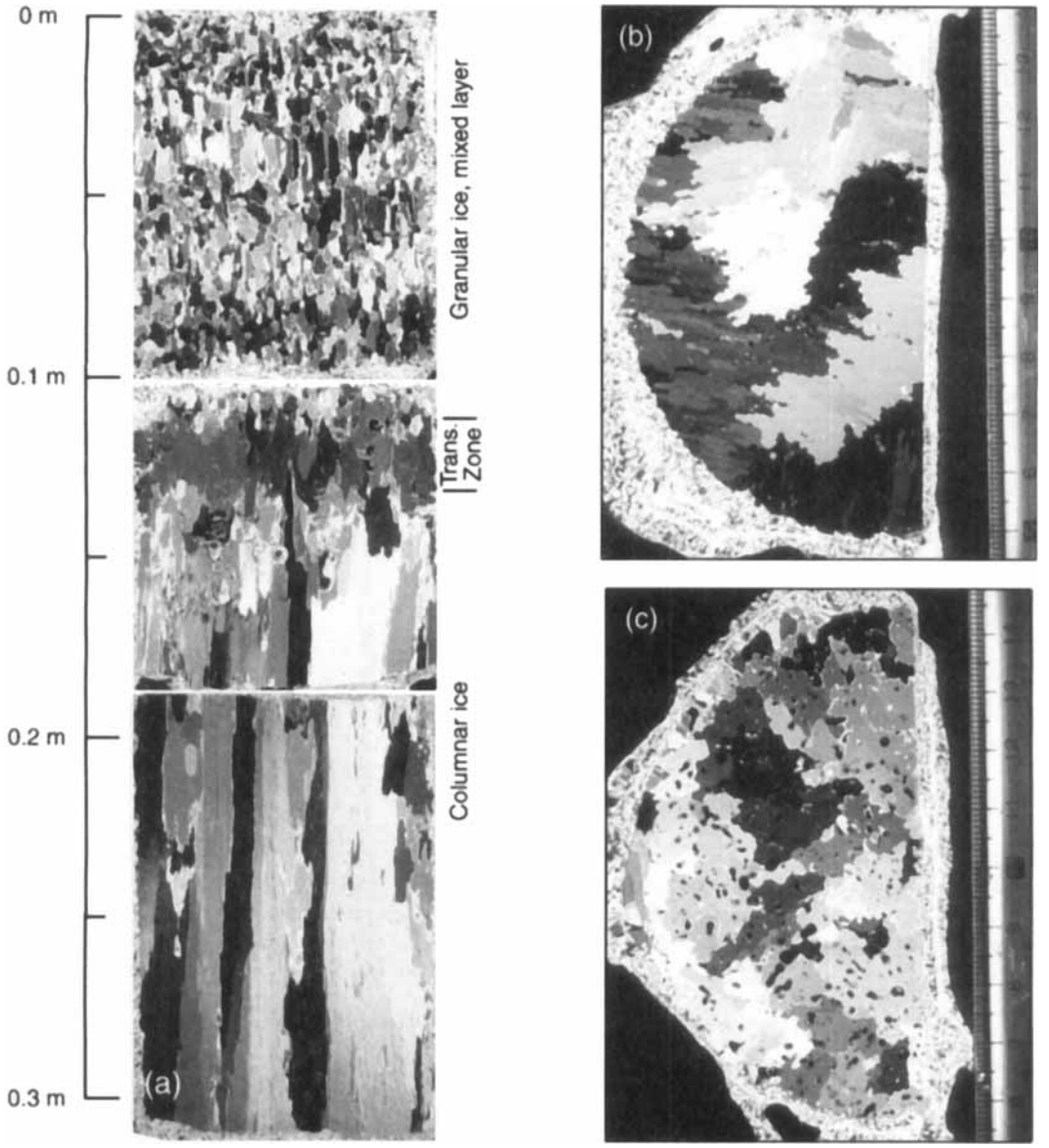

Fig. 4. Thin sections from sea ice cores, photographed between crossed polaroids: (a) combination of three vertical sections of mixed surface layer and columnar ice below, showing the upper 0.3 m of the core (18 May 1997, site DYR), (b) horizontal section of columnar ice (18 May 1997, site DYR), showing relatively large columnar ice crystals, (c) horizontal section of columnar ice (18 June 1997, site BLO), showing relatively large columnar ice crystals with high amount of pores.

snow". The existence of those layers (e.g. Ackley et al. 1979; Lange et al. 1990; Eicken, Lange, Hubberten et al. 1994; Jeffries et al. 1998; Sturm et al. 1998) can be crucial for remote sensing interpretation (e.g. Onstott 1992). The salinity of a melted "refrozen snow" sample (site DYR, 9 June 1998) was 0.40‰, being 11% of the sea ice salinity below. This would indicate superimposed ice (e.g. Onstott 1992) formed by surface melting, percolation and refreezing. It could have been formed in May, under positive freeboard conditions, and temporal air temperatures above 0°C (C. Haas, pers. comm. 1999). In contrast, snow–ice, formed after flooding, gen-

erally exhibits higher salinity than sea ice (Eicken 1998). However, we later observed very wet snow in the snowpack's lower part and negative freeboard, both pointing to flooding. We also observed a positive salinity gradient with depth in the snow, which indicates sea water wicking (e.g. Sturm et al. 1998). These conditions could lead to additional snow–ice formation (Lange et al. 1990).

Texture of sea ice: Laboratory texture analyses were performed on thick and thin sections of vertical and horizontal cuts of two sea ice cores. Thick sections were inspected on a light table in order to detect pores, brine drainage channels and algae, and thin sections between crossed polaroids for visualization of individual crystals (e.g. Gow et al. 1986). A core, taken at DYR on 18 May 1997, exhibited columnar ice with large columnar crystals (length >0.1 m) below a 0.11 m thick mixed surface layer with granular ice and small ice columns (max. crystal length 10 mm), and a ca. 20 mm thick transition zone in between (Fig. 4a). Horizontal thin sections taken from the columnar ice of the cores from 18 May and 18 June 1997 (retrieved at site BLO, ice thickness 0.51 m) show a significant increase in porosity (Figs. 4b, c).

Sea ice algae: After early May 1997 we observed brownish coloured ice in the columnar ice at the lowest section of the cores. The lowermost 40 mm contained algae, attenuating light significantly more than the ice above (Fig. 5). These algae vanished during spring. Living in brine channels between the ice platelets that form very young sea ice, the algae disappear in June as the melt begins and associated conditions, such as water salinity, change (M. Poltermann, pers. comm. 1999). We observed a maximum in the visible sea ice algae development at DYR during the second half of May. Horner (1985) found a similar timing for the Beaufort Sea. Zeebe et al. (1996) modelled the effect of radiation attenuation by an algae bottom layer to be about 90% relative to the incoming radiation above the layer. The algae absorb solar radiation most at wavelengths below 550 nm (Perovich, Cota et al. 1993).

Spectral albedo and under-ice solar radiation: A decrease in albedo at DYR and BLO during spring (Fig. 6a) is mainly due to thinning of the snow cover and snow grain growth. On 18 May 1997,

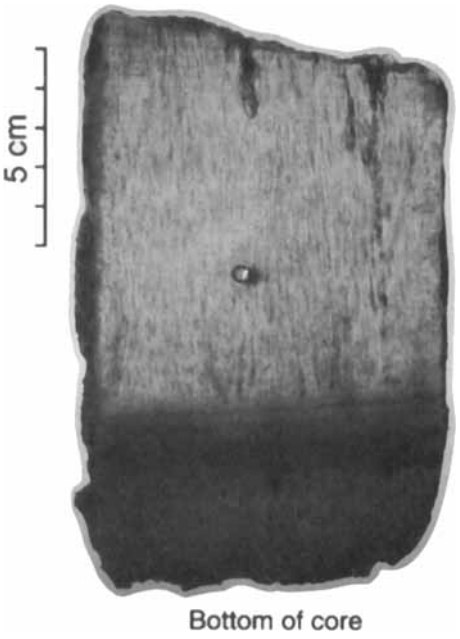

Fig. 5. Thick section of bottom section showing the darkening of the ice by ice algae (18 May 1997, site DYR). The hole in the center of the section was drilled to measure temperature inside the core.

the average snow density was 318 kg m^{-3}, whereas the average snow grain size was 2 mm. The main part of the snow pack appeared relatively dry with only some liquid water at the snow–sea ice interface. On 3 June 1997, the average snow density was 356 kg m^{-3} and the snow grain size at a fresh thin surface layer was 0.5 mm. Below that, snow grains were by then already about 4 mm large. At this stage, the refrozen snow layer formed. On 18 June 1997, melting reached an advanced stage and little snow was left. Snow grains reached sizes of 5 to 10 mm, the surface was wet and melt ponds developed.

Maximum albedo values were about 0.96 on 18 May 1997, while on 3 June and 18 June 1997 they were 0.92 and 0.74, respectively (Fig. 6a). Interestingly, the change in albedo between 18 May and 3 June 1997 mainly occurred in the visible wavelength range, probably due to the darker ice surface shining through the snow layer, and perhaps also some surface blackening from fine dust from nearby moraines. As spring progressed, the snow became both thinner and more transparent (Gerland et al. 1999). From 3 to 18 June 1997, a more pronounced decrease in

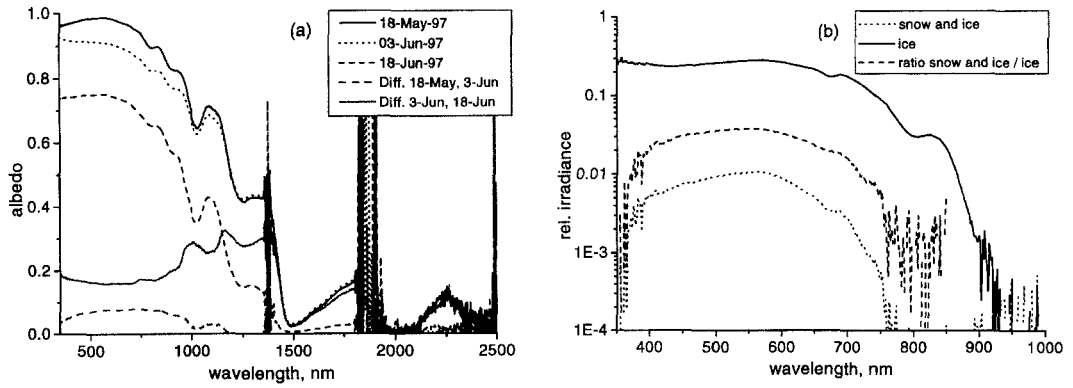

Fig. 6. (a) Surface-reflectance studies (albedo measurements) from early (18 May, site DYR, solid black curve), mid- (3 June, site DYR, dotted black curve) and late (18 June, site BLO, dashed black curve) season 1997. Also plotted is the difference in albedo between 18 May 1997 and 3 June 1997 (dashed gray curve) and between 3 June 1997 and 18 June 1997 (solid gray curve) as a function of wavelength. The sky was clear on all three observation days. (b) Under-ice radiation measurements, taken at DYR on 13 May 1998. Spectral irradiance that reaches the water masses is plotted relative to the irradiance at the surface with snow (dotted curve) and without snow cover (snow was removed, solid curve). The ratio between both curves (dashed curve) is only plotted until 850 nm. Irradiance for individual measurements above that wavelength is very low, and the ratio would be mainly affected by instrument noise.

visible albedo occurred. Even more remarkable was the decrease of near-infrared and infrared albedo during this period, caused by increasing grain sizes and the liquid water in the snow pack.

We performed an experiment measuring under-ice irradiance, both with snow on top of the sea ice and also when the snow was removed from the ice (Fig. 6b). Thus, we were able to distinguish between the attenuation effect from ice and from the combined ice and snow layer. The average snow density was 260 kg m^{-3}, with grain sizes varying from 0.1 to 5 mm (smallest grains at the top). The average snow temperature was −2.8°C, and the thickness 0.21 m. The sea ice thickness was 0.61 m, with temperatures from −3.0°C (top) to −1.5°C (bottom; Fig. 3a). Data were corrected with an immersion correction factor of 1/0.7, which takes different refractions of air and water around the sensors into account. The measurement with snow shows that about 1% of the surface radiation at 550 nm penetrated through the entire snow–sea ice system. After removing the snow, it became obvious that the snow blocks most of the radiation. In this particular case 3.7% of the irradiance at 550 nm penetrated the sea ice with a snow cover on top compared to the situation when snow was removed. This relationship was smaller for shorter and longer wavelengths, e.g. 2.3% at 400 nm and 1.6% at 700 nm (Fig. 6b). Infrared radiation penetrates less deeply into the snow pack than does visible radiation. Here, this is visualized by the near absence of radiation above 750 nm in the case including snow, whereas a significant portion of IR radiation reached the water masses in the case without snow.

Conclusions

Similar ice characteristics observed in two consecutive years indicate that the observed conditions are rather typical for fast ice in spring in Kongsfjorden. The significant reduction of spectral surface albedo during spring, affected by snow thinning and metamorphism, shows how sensitive the sea ice can be to climate change related processes. Moreover, our radiation measurements under the sea ice showed that changes in average snow thickness would heavily affect the amount of optical radiation penetrating the sea ice and thus the amount of radiation available for the ecosystem in and below the ice.

Acknowledgements. – We thank H. Miller, H. Eicken and C. Haas from the Alfred Wegener Institute (AWI) for Polar and Marine Research (Bremerhaven, Germany) for lending us the EM31 instrument. C. Haas (AWI) and M. Poltermann (Norwegian Polar Institute, NP), helped with instructive discussions. Thin and thick section work was done at AWI's cold laboratory with support from F. V. Delgado (AWI). We thank A. Blanco (University of Helsinki) and O.-G. Støen (NP) for their help in the field. This work was performed as part of the project "Spectral Reflective Characteristics of Snow and Sea

Ice", within the Arctic Light and Heat (ALV) Programme, funded by the Norwegian Research Council and NP.

References

Ackley, S. F., Buck, K. R. & Taguchi, S. 1979: Standing crop of algae in the sea ice of the Weddell Sea region. *Deep-Sea Res. 26A*, 269–281.

Clarke, D. B. & Ackley, S. F. 1984: Sea ice structure and biological activity in the Antarctic marginal ice zone. *J. Geophys. Res. 89(C2)*, 2087–2095.

Eicken, H. 1998: Deriving modes and rates of ice growth in the Weddell Sea from microstructural, salinity and stable isotope data. In M. O. Jeffries (ed.): *Antarctic sea ice: physical processes, interactions and variability. Antarct. Res. Ser. 74*. 89–122.

Eicken, H., Lange, M. A. & Dieckmann, G. S. 1991: Spatial variability of sea-ice properties in the Northwestern Weddell Sea. *J. Geophys. Res. 96(C6)*, 10603–10615.

Eicken, H., Lange, M. A., Hubberten, H.-W. & Wadhams, P. 1994: Characteristics and distribution patterns of snow and meteoric ice in the Weddell Sea and their contribution to the mass balance of sea ice. *Ann. Geophys. 12*, 80–93.

Førland, E. J., Hanssen-Bauer, I. & Nordli, P. Ø. 1997: Climate statistics and longterm series of temperature and precipitation at Svalbard and Jan Mayen. *DNMI (Det Norske Meteorologiske Institutt) Klima Rapp. 21*, 72 pp.

Gerland, S., Winther, J.-G., Ørbæk, J. B., Liston, G. E., Øritsland, N. A., Blanco, A. & Ivanov, B. 1999: Physical and optical properties of snow covering Arctic tundra on Svalbard. *Hydrol. Process. 13(14/15)*, 2331–2343.

Gow, A. J., Tucker III, W. B. & Weeks, W. F. 1986: Crystal structure of Fram Strait sea ice. *CRREL Special Report 86(3)/ MIZEX Bulletin VII*, 20–29.

Haas, C. 1998: Evaluation of ship-based electromagnetic-inductive thickness measurements of summer sea-ice in the Bellingshausen and Amundsen seas, Antarctica. *Cold Regions Sci. Technol. 27*, 1–16.

Haas, C., Gerland, S., Eicken, H. & Miller, H. 1997: Comparison of sea-ice thickness measurements under summer and winter conditions in the Arctic using a small electromagnetic induction device. *Geophysics 62(3)*, 749–757.

Horner, R. A. (ed.) 1985. *Sea ice biota*. 215 pp. Boca Raton, FL (USA): CRC Press.

Kovacs, A. & Morey, R. M. 1991: Sounding sea ice thickness using a portable electromagnetic induction instrument. *Geophysics 56(12)*, 1992–1998.

Jeffries, M. O., Li, S., Jana, R. A., Krouse, H. R. & Hurst-Cushing, B. 1998: Late winter first-year ice floe thickness variability, sea water flooding and snow ice formation in the Amundsen and Ross Seas. In M. O. Jeffries (ed.): *Antarctic sea ice: physical processes, interactions and variability. Antarct. Res. Ser. 74*, 69–87.

LaChapelle, E. R. 1992: *Field guide to snow crystals*. Cambridge (UK): International Glaciological Society.

Lange, M. A., Schlosser, P., Ackley S. F., Wadhams, P. & Dieckmann, G. S. 1990. ^{18}O concentrations in sea ice of the Weddell Sea, Antarctica. *J. Glaciol. 36(124)*, 315–323.

Langleben, M. P. 1968: Albedo measurements of an Arctic ice cover from high towers. *J. Glaciol. 7(50)*, 289–297.

Mehlum, F. 1991: Breeding population size of the common eider *Somateria mollissima* in Kongsfjorden, Svalbard, 1981–1987. *Nor. Polarinst. Skr. 195*, 21–29.

Mobley, C. D., Cota, G. F., Grenfell, T. C., Maffione, R. A., Pegau, W. S. & Perovich, D. K. 1998: Modeling light propagation in sea ice. *IEEE Trans. Geosci. Remote Sens. 36(5)*, 1743–1749.

Onstott, R. G. 1992: SAR and scatterometer signatures of sea ice. In F. D. Carsey (ed.): *Microwave remote sensing of sea ice. Geophys. Monogr. 68*, 73–104.

Perovich, D. K. 1994: Light reflection from sea ice during the onset of melt. *J. Geophys. Res. 99(C2)*, 3351–3359.

Perovich, D. K., Cota, G. F., Maykut, G. A. & Grenfell, T. C. 1993: Bio-optical observations of first-year Arctic sea ice. *Geophys. Res. Lett. 20*, 1059–1062.

Perovich, D. K., Roesler, C. S. & Pegau, W. S. 1998: Variability in Arctic sea ice optical properties. *J. Geophys. Res. 103(C1)*, 1193–1208.

Smith, T. G. & Lydersen, C. 1991: Availability of suitable land-fast ice and predation as factors limiting ringed seal populations, *Phoca hispida*, in Svalbard. *Polar Res. 10(2)*, 585–594.

Sturm, M., Morris, K. & Massom, R. 1998: The winter snow cover of the west Antarctic pack ice: its spatial and temporal variability. In M. O. Jeffries (ed.): *Antarctic sea ice: physical processes, interactions and variability. Antarct. Res. Ser. 74*, 1–18.

Vinje, T., Nordlund, N. & Kvambekk, Å. 1998: Monitoring ice thickness in Fram Strait. *J. Geophys. Res. 103(C5)*, 10437–10449.

Wadhams, P. 1994: Sea ice thickness changes and their relation to climate. In O. M. Johannessen et al. (eds.): *The polar oceans and their role in shaping the global environment. Geophys. Monogr. 85*, 337–361.

Warren, S. G. 1982: Optical properties of snow. *Rev. Geophys. Space Phys. 20(1)*, 67–89.

Winther, J.-G., Gerland, S., Ørbæk, J. B., Ivanov, B., Blanco, A. & Boike, J. 1999: Spectral reflectance of melting snow in a high Arctic watershed on Svalbard: some implications for optical satellite remote sensing studies. *Hydrol. Process. 13(12/13)*, 2033–2049.

Wiscombe, W. J. & Warren, S. G. 1980: A model for the spectral albedo of snow. I: pure snow. *J. Atmos. Sci. 37*, 2712–2733.

Zeebe, R. E., Eicken, H., Robinson, D. H., Wolf-Gladrow, D. & Dieckmann, G. 1996: Modeling the heating and melting of sea ice through light absorption by microalgae. *J. Geophys. Res. 101(C1)*, 1163–1181.